

Optimal Design of Multi-Winding Planar Transformers in 1 MHz GaN Multiple-Output Forward Converters*

Dongdong Hu¹, Dongdong Ye², Zhiliang Zhang¹, Binghui He¹, and Xiaoyong Ren¹

¹ Aero-Power Sci-tech Center, Nanjing University of Aeronautics and Astronautics, Jiangsu, P.R.China

² Beijing Institute of Control Engineering, Beijing, P.R.China

{hdd, zlzhang, hebinghui, renxy and chenqh}@nuaa.edu.cn and yedongdong@bice.org.cn

Abstract—It is a serious challenge to find the optimal winding configuration that realizes minimum leakage inductance of the multi-winding planar transformers due to the complex coupling relationship. The proposed idea is to build the mathematical model of leakage magnetic field energy and screen out all possible winding configurations to solve minimum value with Matlab programming. Then, only limited winding configurations need to be simulated in Maxwell, which saves a lot of design efforts. By analyzing the inductance matrix, the leakage inductance of multi-winding planar transformer can be obtained. Then, the optimal winding configuration is solved. A full GaN active clamp forward converter with self-driven SRs is presented. The GaN drive chips for high reliable gate voltage are combined with self-driven scheme. A 16-layer 2-oz prototype with 1 MHz, 100 V input, 5 V/ 6 A and ± 12 V/ 0.83 A outputs was built. The measured leakage inductance matches the simulated results and is limited as low as 0.5% of the magnetic inductance. The full load efficiency is over 86.2% within input voltage range.

Keywords—eGaN HEMTs; active clamp; multiple-output forward converter; synchronous rectification; multi-winding planar transformer

I. INTRODUCTION

Nowadays dc-dc converters are widely used in aerospace applications. The equipments for the communication, control and protection circuits in aerospace need the power supplies with low DC voltages of 3.3 V, 5 V, ± 12 V etc. A multiple-output converter is typically used to convert high bus voltage to multiple low voltages. The typical bus voltage of a satellite power supply is 28 V at present [1]. Considering the front end voltage of a satellite is 100 V, two-stage conversion architecture is normally accepted with the first stage converters to convert 100 V to 28 V as the bus voltage. In order to increase the power density and efficiency to meet the increasing power requirement, the bus voltage will increase to 100 V in the future. Therefore, the bus converters are no longer needed and the satellite power system can be simplified remarkably.

For the satellite applications, the active clamp technique [2] is extensively used in multiple-output converters. Normally, the active clamp forward converters [3] are classified into the high side clamping and the low side clamping. The high side clamping requires the clamping circuit paralleled with the primary winding and needs a floating driver circuit. The low-side clamping requires the clamping circuit paralleled with the main switch and needs a p-channel switch. The self-driven Synchronous Rectifier (SR) technique is usually adopted in low voltage and high current output channels. At present, the

typical switching frequency of the main switch is about 200 to 400 KHz and the MOSFETs are used. In order to shrink the size and weight of the passive components and further improve the power density of the satellite converters, increasing the switching frequency to MHz range is an effective way [4]-[6]. However higher switching frequency may result in higher frequency-dependent loss such as the switching loss, gate drive loss, magnetic loss and AC winding loss and so on.

Adopting new generation of power device enhancement mode Gallium Nitride (eGaN) High Electron Mobility Transistors (HEMTs) will improve the performance of multiple-output converters [7]. Compared to the silicon MOSFETs with the same voltage and current rating, the eGaN HEMTs have many advantages such as lower gate charge, faster switching speed and smaller package with much reduced parasitics. These advantages make the eGaN HEMTs more suitable to MHz dc-dc converters [8]-[10]. Especially to the satellite power converters, the eGaN HEMTs can help to improve the reliability against the radiation in space application. Nevertheless, special attention has to be paid when applying the eGaN HEMTs. The gate drive voltage is restricted less than 6 V. Once the drive voltage exceeds 6 V, the eGaN HEMTs can be damaged, which makes the self-driven of the SRs challenging.

With the increase of switching frequency, the conventional wire-wound transformers [11] that have large leakage inductance and high altitude are no longer suitable. The planar transformers offer good consistency, low altitude, low parasitic parameters [12]-[13] and high repeatability. These advantages make the planar transformers gradually become critical component of high frequency converters. In the optimization process of a planar transformer, the leakage inductance is the key point. Lower leakage inductances produce lower voltage spikes over the fast speeding switches. For two-winding planar transformers, the leakage inductances in the primary and secondary winding can be conveniently optimized by calculating the leakage magnetic field energy. The leakage magnetic field energy is related to Magneto Motive Force (MMF) [14]-[15]. Due to the simple structure and limited winding layers, the optimal winding configuration with minimum leakage inductance can be found by interleaving windings intuitively. The typical result of winding optimization is usually symmetrical interleaving structure. However, this method is not suitable to multi-winding planar transformers. Due to high complexity of multi-winding configuration, the leakage inductance of each winding is hard to calculate theoretically. Considering there are large numbers of winding layers, the possible winding arrangements are enormous. It is hard to reduce the amount of structures and screen out the precise optimal structure manually. More

*This work was supported by National Natural Science Foundation of China (51722702, 51377077), Outstanding Youth Fund of Jiangsu Province

importantly, the output power difference in each winding involves different leakage inductance requirement of the windings accordingly. The winding configurations are far from manually interleaved structures, therefore finding the optimal multi-winding structure with different output power become a tremendous challenge.

The objective of this paper is to propose an optimization algorithm of multi-winding planar transformers. Compared with simply interleaving windings, this optimization combines numerical calculation and FEA simulation and is suitable to multi-winding planar transformers. Meanwhile, the self-driven circuit is proposed for the GaN SR active clamp forward converters, which ensures high reliability drive and high efficiency for the main high current output.

II. OPTIMIZATION PROBLEMS OF MULTIPLE-OUTPUT CONVERTERS

A. GaN Synchronous Active Clamp Forward Multiple-output Converter

Fig. 1 gives the schematic of the active clamp forward converter. Table I lists the specifications. Compared with the multiple-output forward converter, the duty ratio can exceed 50% and bidirectional magnetization can be realized in the active clamp forward multiple-output converter. In Fig. 1, the converter uses an auxiliary winding to implement the active clamp. The auxiliary circuit consists of a clamping switch and a clamping capacitor. The advantage is that the main and clamping switches are driven conveniently and reliably without the floating driver circuits.

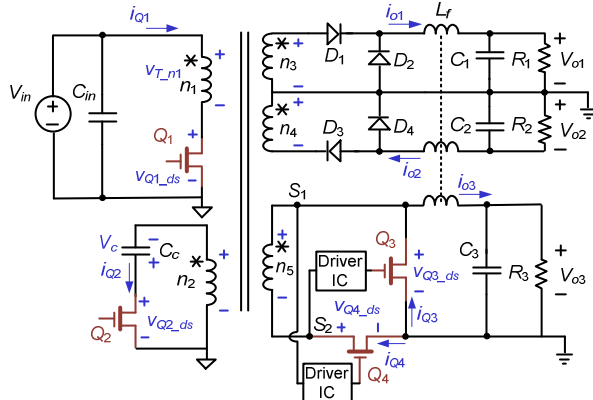


Fig. 1 GaN synchronous active clamp forward multiple-output converter

Table I CONVERTER SPECIFICATIONS

	Voltage (V)	Current (A)	Power (W)
Input	90-110	-	-
Main output	5	6 (high current)	30
Output 1	+12	0.83 (low current)	10
Output 2	-12	0.83 (low current)	10

Considering the main output is 5 V/ 6 A, the self-driven SR is adopted to reduce the conduction loss. Compared with the conventional self-driven MOSFET SR, the eGaN HEMTs need extra driver IC to realize SR. The reason is that the drive signals obtained from the transformer winding exceed the

maximum gate voltage rating of eGaN HEMTs. In order to guarantee the safety drive voltage, a drive chip is adopted here to drive eGaN HEMTs. The other two output channels only need to provide low output current, so the schottky diodes are used. All the active switches in this converter are eGaN HEMTs and the switching frequency is targeted as 1 MHz.

B. Optimization Problems of Multi-winding Planar Transformer

In consideration of achieving high power density, the multi-winding planar transformer has been adopted in the active clamp forward converter. A general method is to analyze the MMF distribution of windings in the window and calculate the leakage magnetic field energy of the transformer theoretically. According to the relationship given in (1) between the leakage inductance and leakage magnetic field energy, the theoretical leakage inductance value is solved.

$$E_{\text{energy}} = \frac{1}{2} \int_{\text{window area}} BHdV = \frac{1}{2} L_{lk} I_p^2 \quad (1)$$

where L_{lk} is the leakage in primary side, I_p is the current of primary winding, B is the magnetic induction intensity in the window and H is the magnetic field strength in the window.

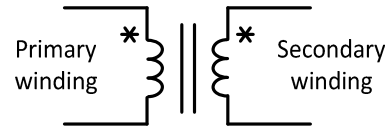


Fig. 2 Two winding transformer

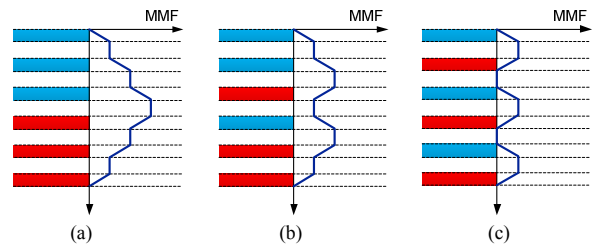


Fig. 3 (a) Non-interleaving structure (b) Part-interleaving structure (c) Interleaving structure

The situation is totally different in multiple-output converters. The main challenge is the design and optimization of planar transformer. Finding the optimal winding arrangement is the key point.

In the multi-winding planar transformer, there are usually three or four windings and even more with auxiliary windings for the power of the control circuit sometimes. Due to different output voltage and power, the turns and current of these secondary windings are different. The magnetic field and coupling relationship of a multi-winding planar transformer is more complex than a two-winding transformer. It is difficult to interleave one primary winding and several secondary windings manually to find the optimal arrangement compared with a simple two-winding transformer. More importantly, the reduction priority of the leakage inductance in the multi-windings is different. For example, 5 V output channel has low output voltage and high output current. The driving signals of SRs are taken from transformer winding. To ensure the SRs operate efficiently, the leakage inductance in this channel should be minimized as first priority during the design trade-off.

III. PROPOSED OPTIMAL DESIGN OF MULTI-WINDING PLANAR TRANSFORMER

The goal of the algorithm is to find the optimal winding configuration from tens of thousands of possible winding structures. This proposed method combines numerical analysis and FEA simulation. The key point of this algorithm is to screen out a few structures that have low leakage magnetic field energy in numerical analysis step and then model these structures in Maxwell to obtain the inductance matrixes, from which the leakage inductance of each winding can be calculated. By sorting all the structures by the priority of the leakage inductance of each winding, the optimal winding structure can be figured out.

A. Numerical Analysis Step

In numerical analysis step, due to the complex coupling relationship between the windings, the calculation formula (1) used in the simply two-winding transformers cannot be applied to the multi-winding structure here directly. However the magnitude of leakage magnetic field energy still reveals the magnitude of the leakage inductance.

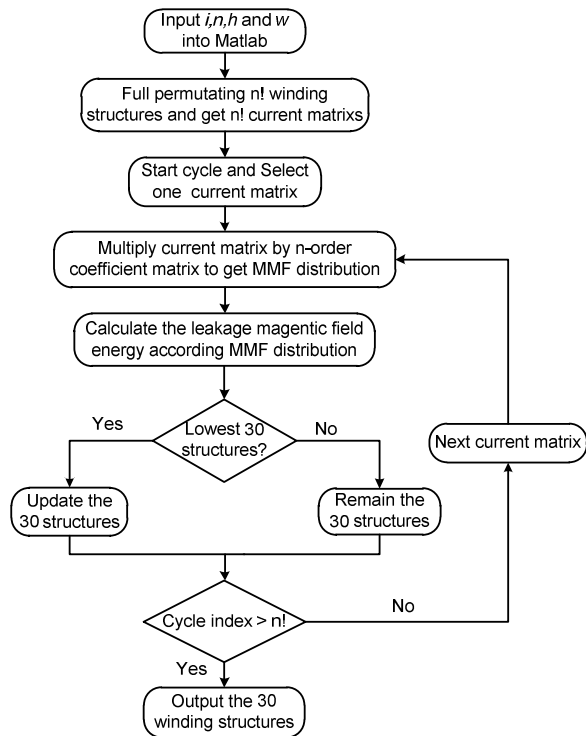


Fig. 4 Flow chart of numerical analysis

Considering the number of layers in multi-winding planar transformer is large, the total amount of winding configurations is large as well. The amount of all the cases is full permutation of all layers. If the number of layers is more than 15, the total amount of all the cases is about 10^8 . The complete calculation cannot be finished manually. With Matlab programming, a large number of cases that have high leakage energy can be filtered out. Fig. 4 gives the flow chart of proposed numerical analysis. By doing this the number of cases can be reduced to about 30. This procedure can improve the screening efficiency and save a lot of design effort.

We need to input parameters of multi-winding planar transformer. The current in each winding, the copper thickness h , the interlayer spacing w and total layers n should be input into Matlab. Then through full permuting all n layers, we can get $n!$ winding structures which correspond to $n!$ current matrixes.

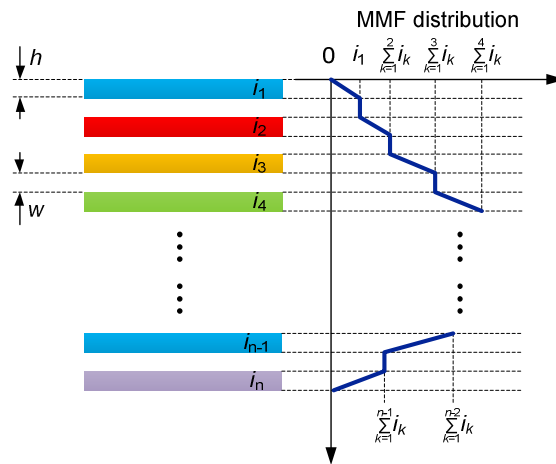


Fig. 5 MMF distribution of winding structure

In equation (2), $i_1, i_2, i_3, \dots, i_n$ represent the current in each layer. Considering the copper thickness and interlayer spacing, we can get a coefficient matrix K . Matrix A equals to matrix I multiply by coefficient matrix, The leakage magnetic field energy is related to the sum of all elements in the matrix A as shown in (4).

$$I = [i_1, i_2, i_3, \dots, i_n] \quad (2)$$

$$K = \begin{bmatrix} \frac{h}{2} + w & h + w & h + w & \dots & h + w \\ 0 & \frac{h}{2} + w & h + w & \dots & h + w \\ 0 & 0 & \frac{h}{2} + w & \dots & h + w \\ \vdots & \vdots & \vdots & \ddots & \vdots \\ 0 & 0 & 0 & \dots & \frac{h}{2} + w \end{bmatrix}_{n \times n} \quad (3)$$

$$A = I \cdot K \quad (4)$$

$$E_{leakage} = \sum_{i=1}^n a_i \quad (5)$$

$$\begin{pmatrix} v_1 \\ v_2 \\ v_3 \\ v_4 \end{pmatrix} = \begin{pmatrix} L_{11} & M_{12} & M_{13} & M_{14} \\ M_{21} & L_{22} & M_{23} & M_{24} \\ M_{31} & M_{32} & L_{33} & M_{34} \\ M_{41} & M_{42} & M_{43} & L_{44} \end{pmatrix} \frac{d}{dt} \begin{pmatrix} i_1 \\ i_2 \\ i_3 \\ i_4 \end{pmatrix} \quad (6)$$

where L_{11}, L_{22}, L_{33} and L_{44} represent self-inductance in the inductance matrix. $M_{12}, M_{13}, M_{14}, M_{23}, M_{24}$ and M_{34} represent mutual-inductance in the inductance matrix.

B. Finite Element Analysis Step

In finite element analysis part, we set models for the selected cases. With the help of Maxwell, we can get the self- and mutual- inductances matrix as shown in equation (6). Then the leakage inductance of each winding can be calculated theoretically. We can sort all the cases by the priority of leakage inductance request of each winding and pick out the optimal winding configuration.

When the inductance matrix is obtained, the leakage inductance of each winding in different situations can be calculated. For example, the leakage inductance of primary winding can be calculated when other windings are shorted. In (6), the relationship of voltage and current in each winding is up to the inductance matrix L . By using Laplace Transform, the results are simplified. The relationship of i versus v can be calculated by matrix operation. In (8), the matrix G is the inverse of matrix L .

In order to find out the leakage inductance, the equivalent voltages of different windings need to be set. For example the leakage inductance of primary side can be conveniently obtained by setting $v_2=v_3=v_4=0$ and $v_1=1$. Then the leakage inductance of primary winding is $1/G_{11}$. In the same way, the leakage inductances of other windings can be calculated. These calculated results can be verified in the prototype.

$$L = \begin{pmatrix} L_{11} & M_{12} & M_{13} & M_{14} \\ M_{21} & L_{22} & M_{23} & M_{24} \\ M_{31} & M_{32} & L_{33} & M_{34} \\ M_{41} & M_{42} & M_{43} & L_{44} \end{pmatrix} \quad (7)$$

$$G = L^{-1} \quad (8)$$

$$\begin{pmatrix} i_1 \\ i_2 \\ i_3 \\ i_4 \end{pmatrix} = \frac{1}{s} \cdot \begin{pmatrix} G_{11} & G_{12} & G_{13} & G_{14} \\ G_{21} & G_{22} & G_{23} & G_{24} \\ G_{31} & G_{32} & G_{33} & G_{34} \\ G_{41} & G_{42} & G_{43} & G_{44} \end{pmatrix} \cdot \begin{pmatrix} v_1 \\ v_2 \\ v_3 \\ v_4 \end{pmatrix} \quad (9)$$

Considering the current in the auxiliary winding is very low, the MMF distribution will not be influenced by auxiliary winding. By comparing the leakage inductance of different structures, the structures that have low leakage inductance in 5 V output channel and primary side circuit are selected in first priority. The optimal structure is selected from the 30 cases finally.

IV. SIMULATION OF THE MULTI-WINDING PLANAR TRANSFORMER

A. Numerical Analysis of Winding Configuration

According to the input and output parameters in the Table I, the specifications of the multi-winding planar transformer are given in Table II. The core size is EE14 and the material is 3F45 that has low iron loss in 1 MHz.

The number of layers in multi-winding planar transformer is 16. According to the algorithm proposed in section III, in this process of selecting, turns and current of each winding, the copper thickness in each layer and the distance between two layers will be loaded into Matlab. The total quantity is about 10^8 . Fig. 6 gives the quantity distribution of cases with leakage magnetic field energy. In the low leakage magnetic field energy region we can easily choose about 30 cases starting from the lowest energy.

Table II PLANAR TRANSFORMER SPECIFICATIONS

	Turns	Layers
Primary	24	6
5 V	3	4
+12 V	7	2
-12 V	7	2
Auxiliary	7	2

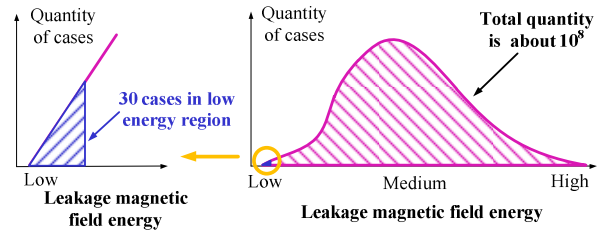


Fig. 6 Quantity distribution of cases with different leakage magnetic field energy

B. FEA Simulation Analysis of Winding Configuration

Considering the current in the auxiliary winding is very low, magneto motive force (MMF) distribution will not be influenced enormously. The selected winding arrangements will be modeled in Maxwell.

We can get self- and mutual-inductance of these cases, then the leakage inductance can be calculated by the method mentioned above. By comparing the leakage inductance of different structures, we can give preference to select the structure that has lowest leakage inductance in 5v output circuit and primary side circuit. Fig. 7 gives the 3D model of selected multi-winding transformer. There are five windings in this planar transformer. The red winding is primary winding and the pink one is auxiliary winding. In secondary side, the 5 V winding is gray and $\pm 12V$ windings are green and blue.

Fig. 8 shows the simulated self- and mutual-inductance matrix. Fig. 9 gives the optimal winding and MMF distribution. The left part is the winding structure and the right part is the MMF distribution. Colors of each winding correspond to the 3D model in Fig. 7. The total number of layers is 16. The copper thickness is selected to be $70\mu\text{m}$ (2 oz) and the interlayer spacing is about $90\mu\text{m}$. The current direction in each winding has been pointed out.

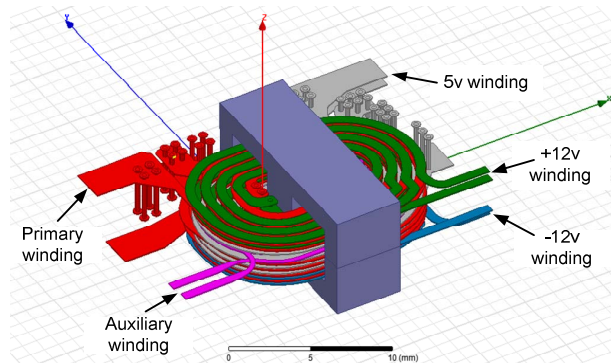


Fig. 7 3D model of multi-winding planar transformer

	Current2	Current6	Current8	Current4
Current2	114.17	33.101	33.351	14.241
Current6	33.101	9.9625	9.4864	4.1093
Current8	33.351	9.4864	10.038	4.1547
Current4	14.241	4.1093	4.1547	1.7956

Fig. 8 Simulated self- and mutual-inductance matrix

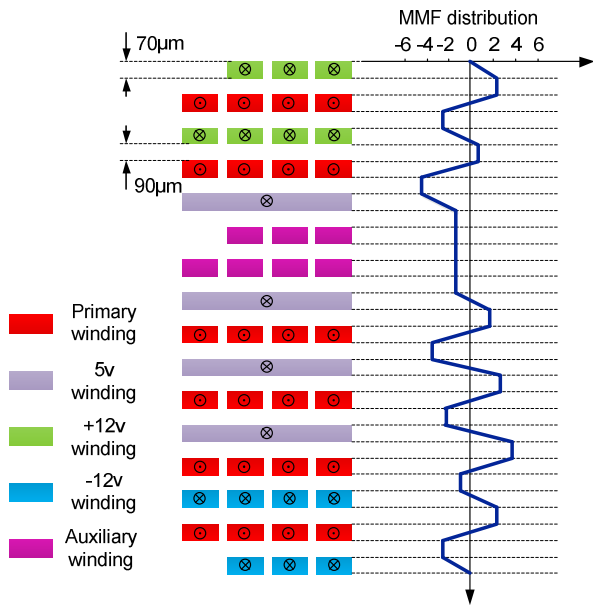


Fig. 9 The optimal winding and MMF distribution

We can get self-and mutual-inductance of these cases, then the leakage inductance can be calculated by the method mentioned above. By comparing the leakage inductance of different structures, we can give preference to select the structure that has lowest leakage inductance in 5v output circuit and primary side circuit.

Table III gives the simulated results. L_{lp} represents the leakage inductance in the primary side while the secondary side windings are all shorted. L_{ls3} represents the leakage inductance in 5 V output channel while the primary winding and ± 12 V circuit windings are all shorted. L_{ls1} and L_{ls2} represent the leakage inductance in ± 12 V circuit when other windings are shorted.

Table III SIMULATED LEAKAGE INDUCTANCE OF EACH WINDING AT 1 MHz

	L_{lp} (primary winding)	L_{ls1} (+12 V output)	L_{ls2} (-12 V output)	L_{ls3} (5 V output)
Simulated results	0.51 uH	0.27 uH	0.30 uH	18 nH

V. EXPERIMENTAL RESULTS AND DISCUSSION

An experimental prototype operating at 1 MHz, 100 V input and 5V/6A and ± 12 V/0.83A output was built. Fig. 10 gives the photograph of the prototype. Table IV lists the component values of multiple-output converters. The windings are composed of two pieces of PCB board and the total number of layers is 16. The copper thickness is selected to be 70 μ m (2 oz) and the interlayer spacing is about 90 μ m.

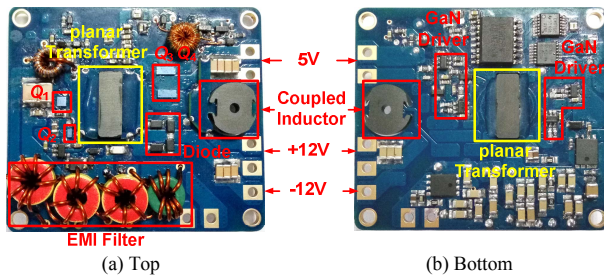


Fig. 10 Photograph of the prototype

Table IV COMPONENTS IN THE MULTIPLE-OUTPUT CONVERTER

Q_1	EPC2025 (EPC) (300V/4A, eGaN)	$n_1:n_2:n_3:n_4:n_5$	24:7:7:3
Q_2	EPC2012C (EPC) (200V/5A, eGaN)	Diode	PMEG10020ELR (NXP)
Q_3, Q_4	EPC2015C (EPC) (40V/36A, eGaN)	Core	EE14/3.5/5(3F45)

Table V gives the comparison of simulated and experimental results. In simulated results, the percentage of leakage inductance in primary side is about 0.5% and the percentage of leakage inductance in 5v output circuit is about 1%. In experimental results, the corresponding two percentages are about 0.59% and 1.5%.

Table V TESTED LEAKAGE INDUCTANCE OF PROTOTYPE

	L_{lp} (uH)	L_{ls1} (uH)	L_{ls2} (uH)	L_{ls3} (uH)
Simulated results	0.51	0.27	0.30	0.018
Experimental results	0.65	0.35	0.37	0.025

Fig. 11 and Fig. 12 show the drain and gate voltage waveforms of the control FET and clamping FET. It is observed that the drain voltage is approximately 250 V at 100V input. The peak drain voltage of clamping FET is 130 V at 100 V input.

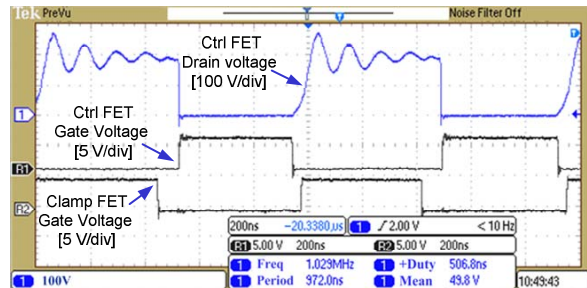


Fig. 11 Waveforms of the control FET Q_1 :

$V_{in}=100$ V, $V_{o3}=5$ V, $I_{o3}=6$ A, $V_{o1}=+12$ V, $I_{o1}=0.83$ A, $V_{o2}=-12$ V, $I_{o2}=0.83$ A and $f_s=1$ MHz

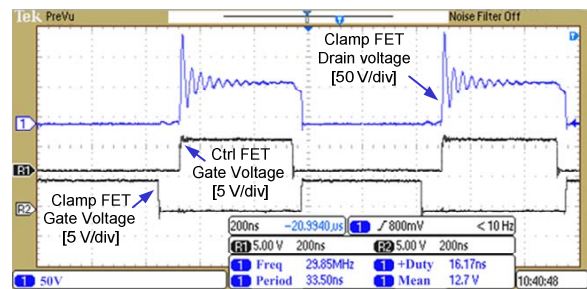


Fig. 12 Waveforms of the clamping FET Q_2 :

$V_{in}=100$ V, $V_{o3}=5$ V, $I_{o3}=6$ A, $V_{o1}=+12$ V, $I_{o1}=0.83$ A, $V_{o2}=-12$ V, $I_{o2}=0.83$ A and $f_s=1$ MHz

The efficiency was measured with the optimal multi-winding planar transformer. Fig. 13 gives the loss distribution of the multi-output forward converter. Fig. 14 gives the efficiency curve with the different input voltage. The

efficiency is above 86.2% among the input voltage range owing to the low leakage inductance.

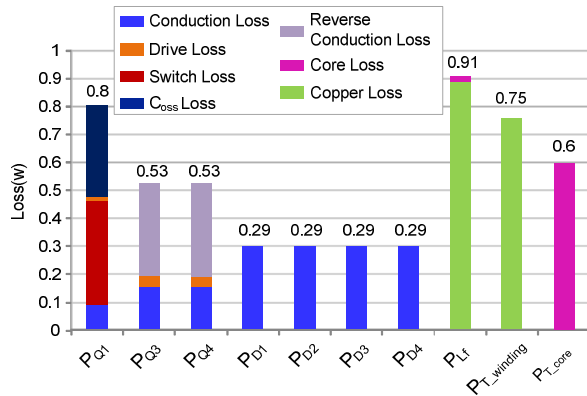


Fig. 13 Loss distribution of multi-output forward converter

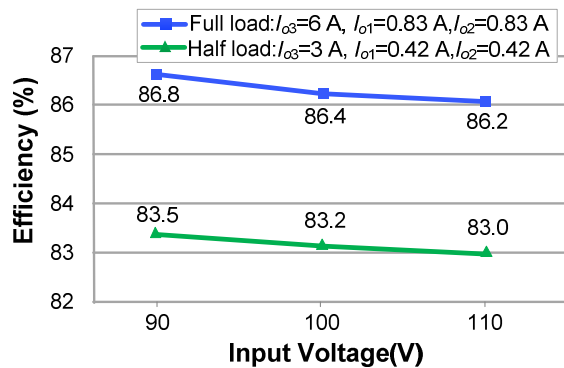


Fig. 14 Efficiency curve at different input voltage:
 $V_{o3}=5\text{ V}$, $V_{o1}=+12\text{ V}$, $V_{o2}=-12\text{ V}$ and $f_s=1\text{ MHz}$

VI. CONCLUSION

This paper focuses on how to achieve optimal design of a planar multi-winding transformer with the asymmetrical turns and currents of each winding. Due to the complex coupling relationship in the multi-winding planar transformers, finding the optimal winding configuration that has minimum leakage inductance is a serious challenge. An algorithm that combines numerical calculation and FEA simulation to screen out optimal suitable configuration is proposed. Compared with simply interleaving primary and secondary windings in two-winding transformers, this method can realize the traversal of all possible configurations by Matlab and search out the optimal configuration according to the leakage inductance request of windings with different output voltage and power. Compared with the conventional self-driven method, the GaN drive chip for high reliable gate voltage is combined with self-driven scheme to drive the SR GaN

HEMTs. The results show the leakage inductances in the main output channel with high current should be minimized as priority. This method was applied to optimize a multi-winding planar transformer. An experimental prototype with 1 MHz, 100 V input, 5 V /6 A and $\pm 12\text{ V}/0.83\text{ A}$ output was built to verify the proposed method. The optimized efficiency with full load is over 86.2% within input voltage range. The measured leakage inductance matches the simulated result well and is only as low as 0.5% of the magnetic inductance.

REFERENCES

- [1] K. S. Low and C. Zheng, "Virtual instrument for a micro-satellite power supply system," in *Proc. IEEE IMTC—Special Session on Space Frontiers of Measurement.*, May 1–3, 2007, pp. 1–6.
- [2] P. Jang and B. H. Cho, "Two-switch forward converter with reset winding and an auxiliary active-clamp circuit for a wide input voltage range," in *IEEE Transactions on Power Electronics*, vol. 32, no. 6, pp. 4491–4502, June 2017.
- [3] F. D. Tan, "The forward converter: From the classic to the contemporary," in *Proc. IEEE APEC*, vol. 2, pp. 857–863, Mar. 2002.
- [4] D. J. Perreault, J. Hu, J. M. Rivas, Y. Han, O. Leitermann, R. C. N. Pilawa-Podgurski, A. Sagneri, and C. R. Sullivan, "Opportunities and challenges in very high frequency power conversion," in *Proc. IEEE APEC*, pp. 1–14, Feb. 2009.
- [5] X. Ren, Yuan Zhou, D. Wang, X. Zou and Zhiliang Zhang, "A 10-MHz isolated synchronous Class- $\Phi 2$ resonant converter," *IEEE Trans. Power Electron.*, Vol. 31, No. 12, pp. 8317–8328, Dec. 2016.
- [6] Z. Zhang, X. W. Zou, Y. Zhou, Z. Dong and X. Ren, "A 10-MHz eGaN isolated Class- $\Phi 2$ DCX," *IEEE Trans. Power Electron.*, Vol. 32, No. 3, pp. 2029–2040, Mar. 2017.
- [7] S. L. Colino and R. A. Beach, "Fundamentals of gallium nitride power transistors," Application Note, EPC Co., 2010.
- [8] Y. Wang, W. Kim, Z. Zhang, J. Calata, and K. D. T. Ngo, "Experience with 1 to 3 megahertz power conversion using eGaN FETs," in *Proc. IEEE APEC*, 2013, pp. 532–539.
- [9] Z. Zhang, Z. Dong, X. W. Zou, D. Hu, and X. Ren, "A digital adaptive driving scheme for eGaN HEMTs in VHF converters," *IEEE Trans. Power Electron.*, Vol. 32, No. 8, pp. 6197–6205, 2017.
- [10] Z. Zhang, Z. Dong, D. D. Hu, X. W. Zou, and X. Ren, "Three-level gate drivers for eGaN HEMTs in resonant SEPIC converters," *IEEE Trans. Power Electron.*, Vol. 32, No. 7, pp. 5527–5538, 2017.
- [11] Z. Ouyang and M. A. E. Andersen, "Overview of planar magnetic technology fundamental properties," in *IEEE Trans. Power Electron.*, vol. 29, no. 9, pp. 4888–4900, Sep. 2014.
- [12] M. A. Saket, N. Shafiei, M. Ordenez, M. Craciun, and C. Botting, "Low parasitics planar transformer for LLC resonant battery chargers," in *Proc. IEEE APEC*, 2016, vol. 1, pp. 854–858, Mar 2016.
- [13] M. A. Saket, N. Shafiei, and M. Ordenez, "Planar transformer winding technique for reduced capacitance in LLC power converters," in *Proc. Energy Conversion Congress and Exposition (ECCE)*, IEEE, pp. 1–6., 18–22 Sep 2016.
- [14] J. H. Jung and S. Ahmed, "Flyback converter with novel active clamp control and secondary side post regulator for low standby power consumption under high-efficiency operation," *IET Power Electron.*, vol. 4, no. 9, pp. 10581067, Nov. 2011.
- [15] J. Zhang, Z. Ouyang, M. C. Duffy, M. A. E. Andersen, and W. G. Hurley, "Leakage inductance calculation for planar transformers with a magnetic shunt," *IEEE Trans. Ind. Application.*, vol. 50, no. 6, pp. 4107–4112, Nov.-Dec. 2014.